Hindawi Publishing Corporation
Journal of Nanomaterials
Volume 2012, Article ID 325605, 8 pages
doi:10.1155/2012/325605

Research Article

Understanding the Biocompatibility of Sintered Calcium Phosphate with Ratio of [Ca]/[P] = 1.50

Feng-Lin Yen,[1] Wei-Jen Shih,[2] Min-Hsiung Hon,[3] Hui-Ting Chen,[1] I-Ming Hung,[4] Homg-Huey Ko,[1] and Moo-Chin Wang[1]

[1] *Department of Fragrance and Cosmetic Science, Kaohsiung Medical University, 100 Shih-Chuan 1st Road, Kaohsiung 80782, Taiwan*
[2] *Medical Devices and Opto-Electronics Equipment Department, Metal Industries Research and Development Center, 1001 Kaonan Highway, Kaohsiung 81160, Taiwan*
[3] *Department of Materials Science and Engineering, National Cheng Kung University, 1 Ta-Hsueh Road, Tainan 70101, Taiwan*
[4] *Department of Chemical Engineering and Materials Science, Yuan Ze University, 135 Yuan-Tung Road, Chungli, Taiyunn 320, Taiwan*

Correspondence should be addressed to Moo-Chin Wang, mcwang@kmu.edu.tw

Received 3 September 2012; Revised 13 October 2012; Accepted 15 October 2012

Academic Editor: Yan-Yan Song

Biocompatibility of sintered calcium phosphate pellets with [Ca]/[P] = 1.50 was determined in this study. Calcium pyrophosphate (CPP) phase formed on the sintered pellets immersed in a normal saline solution for 14 d at 37°C. The intensities of hydroxyapatite (HA) reflections in the X-ray diffraction (XRD) patterns of the pellets were retrieved to as-sintered state. The pellet surface morphology shows that CPP crystallites were clearly present and make an amorphous calcium phosphate (ACP) to discriminate against become to the area of slice join together. In addition, the intensities of the CPP reflections in the XRD patterns were the highest when the pellets were immersed for 28 d. When the CPP powders were extracted from the pellets after immersion in the solution for 14 d, the viability of 3T3 cells remained above 90% for culture times from 1 to 4 d. The pellet surface morphology observed using optical microscopy showed that the cells did not adhere to the bottom of the sintered pellets when cultured for 4 d; however, some CPP phase precipitates were formed, as confirmed by XRD. In consequence, the results suggest that the sintered HA powders are good materials for use in biomedical applications because of their good biocompatibility.

1. Introduction

Among calcium phosphate-based ceramics, hydroxyapatite (HA, $Ca_{10}(PO_4)_6(OH)_2$) and β-tricalcium phosphate (β-TCP, β-$Ca_3(PO_4)_2$) are the most commonly used as bioresorbable materials and tissue-engineering scaffolds [1–3] because these ceramics are biocompatible, nontoxic, and resorbable, and because they exhibit excellent osteoconductive ability. HA has widely been used as bone cement and implant material for direct bone-to-bone grafts [4–6]. Nevertheless, natural bone is a nanocomposite combination consisting of an organic fraction and a mineral fraction containing a small amount of apatite crystals and nonstoichiometric calcium phosphate, which jointly confer mechanical resistance [7]. Therefore, applications of HA are currently limited to powders, coatings, porous bodies, and non-load-bearing implants owing to process difficulties and to the poor mechanical properties of conventional HA also reported by Suchanek and Yoshimura [8].

Prepared nanosized HA has received much attention in recent years for simulating natural structures [9–11]. Nanoscale-engineered HA would exhibit amazing functional properties owing to its small crystallite size, large surface area to volume ratio, and ultrafine structure similar to that of biological apatite, which would have a great effect on the interaction of cells implanted in the body. In addition, the nanoscale particle size and morphology of HA can control the sinterability, solubility, mechanical reliability, and osteoconductivity of HA [12, 13]. It is important to investigate methods of fabricating HA powders at low temperature such as sol-gel [14, 15], salt hydrolysis [16–18], electrochemical deposition [19–23], microemulsion [24], microwave irradiation [25], and hydrothermal reaction [26]. Using wet chemical methods to prepare HA powders usually

results in fine-grained microstructures, even submicron- to nanocrystallites, which are better accepted by the host tissue.

Although HA powders have previously been fabricated using calcium hydrogen phosphate dihydrate ($CaHPO_4 \cdot 2H_2O$, DCPD) and calcium carbonate ($CaCO_3$) as starting materials with hydrolysis [12], calcium-deficient HA (d-HA, $Ca_{10-x}(HPO_4)_x(PO_4)_{6-x}(OH)_2 \cdot nH_2O$, for $0 \le x \le 1$) was formed, and there was significant lattice disparity between $Ca_{20}Na_{2x}(P_2O_7)_{1-x}(PO_4)_{12+2x}$ and $Ca_{10-x}Na_x(PO_4)_{6-x}(CO_3)_{1+x}$ at calcination temperatures from 600 to 1000°C. The arrangements of phosphate in the structure give two different channels for calcium atoms under two different environments [26]. The phosphate or hydroxyl groups can be substituted with carbonate species [27]. When the d-HA powders are sintered above 800°C, on the other hand, a small amount of rhenanite ($CaNaPO_4$) phase is formed with the HA. The sintered HA must first be put through the immersion test to determine the biocompatibility of sintered calcium phosphate prepared in a ratio of [Ca]/[P] = 1.50.

In the present study, variations in the surfaces of sintered calcium phosphate pellets prepared in a ratio of [Ca]/[P] = 1.50 and immersed in a normal saline solution at 37°C were observed and the biocompatibility of calcium phosphate powders and the sintered pellets were investigated. The main purposes of this work were to: (i) understand the surface transition behavior of the sintered calcium phosphate pellet prepared in a ratio of [Ca]/[P] = 1.50 and immersed in a normal saline solution for various of time, (ii) study the mechanism of dissolution and changes in the properties of sintered the calcium phosphate pellet after it has been immersed in culture medium for various time, (iii) determine the biocompatibility of calcium phosphate powders prepared in a ratio of [Ca]/[P]= 1.50, and (iv) study the biocompatibility of the sintered calcium phosphate pellet prepared in the ratio of [Ca]/[P] = 1.50.

2. Experimental Procedure

2.1. Sample Preparation. In the present study, calcium hydrogen phosphate dihydrate ($CaHPO_4 \cdot 2H_2O$, DCPD, purity ≥98%, Riedel-de Häen, Germany) and calcium carbonate ($CaCO_3$, purity ≥98.5%, Riedel-de Häen, Germany) were used as the starting materials. First, either 0.1 M DCPD was mixed with $CaCO_3$ in a ratio of [Ca]/[P] = 1.50 or pure DCPD was poured into a 500 mL NaOH solution (pH = 13, purity ≥99%, Showa Co., Japan). The mixtures were blended separately in a high-speed agitator at 75°C for 1 h. After hydrolysis, the reactions were stopped by cooling the reaction mixtures in ice water. The precipitate products were filtered and then rinsed in deionized water. The products were subsequently dried at 60°C and sieved with a 300 mesh until further use.

The synthesized powder prepared in a ratio of [Ca]/[P] = 1.50 was used as received without any binders added. Each sample consisted of 0.25 g of synthesized powder uniaxially cool-pressed at 23 MPa to form a 10 mm ϕ pellet. The pellets were then sintered by heating them from 25 to 800°C at a rate of 2°C/min for 4 h in air. After all the samples were sintered, they were removed from the furnace and were cooled in air.

2.2. Sample Characterization. X-ray diffraction (XRD) analysis on the crystalline phase of the as-dried and sintered samples was performed before and after they were immersed in normal saline solution at 37°C for various amounts of time. The analysis was performed using an X-ray diffractometer (Rigaku D-Max/III, Tokyo, Japan) with monochromatic Cu-Kα radiation ($\lambda = 1.5405$ Å) and a Ni filter. The operation voltage and current were 30 kV and 20 mA at a scanning rate (2θ) of 1°/min.

The surface morphology of the sintered pellets was observed using scanning electron microscopy (SEM, Model XL 40 FE-SEM, Philips, Eindhoven, Netherlands). After the sintered pellets had been immersed in the normal saline solution at 37°C for various times, they were freeze dried at −55°C in vacuum and were then coated with gold.

The Ca^{2+} concentration was detected using inductively coupled plasma-mass spectrometry (ICP-MS). An ELAN 6100 DRC II ICP-MS (Perkin-Elmer, Concord, ON, Canada) was used for these experiments. Samples were introduced using a pneumatic nebulizer with a Scott spray chamber. The operating conditions of ICP-MS were optimized by continuously introducing saline solution after the immersed calcium phosphate samples containing unknown Ca^{2+} concentrations). The unused saline was treated as the blank and was added to the standard solution used to produce a calibration curve. The solution flow rate was maintained at about 1.5 mL·min^{-1}.

2.3. Determination of Biocompatibility with 3T3 Cells. The calcium phosphate powder pellets prepared in a ratio of [Ca]/[P] = 1.50 were sterilized and immersed in a culture medium for 4, 7, 14, or 21 d at 37°C. The resulting media were then used to culture 3T3 fibroblasts. About 1×10^4 3T3 cells in 100 μL of immersion medium were seeded into each well of a 96-well culture plate and were cultured for 1, 2, 3, or 4 d. Cell viability was determined using MTT (3-(4,5-dimethylthiazol-2-yl)-2,5-diphenyltetrazolium bromide) assay. In addition, the sintered pellet of calcium phosphate prepared in the ratio of [Ca]/[P] = 1.50 was placed into an 80 mm dish and immersed in 75% alcohol for sterilization. After 24 h, the residual alcohol on the sintered pellet was removed by washing the pellet with the culture medium. The washed sintered pellet was then immersed in the culture medium. About 1×10^4 3T3 cells were seeded onto the sintered pellet and were incubated in a 5% CO_2 atmosphere for 4 d at 37°C so that the cells could adhere to the pellet. The morphology of the cells adhered to sintered pellet was observed with an optical microscope and scanning electron microscopy.

3. Results and Discussion

3.1. Transition on Surface of Sintered Calcium Phosphate Pellet Prepared in a Ratio of [Ca]/[P] = 1.50 and Immersed in Normal Saline Solution. Figure 1 shows the XRD patterns for

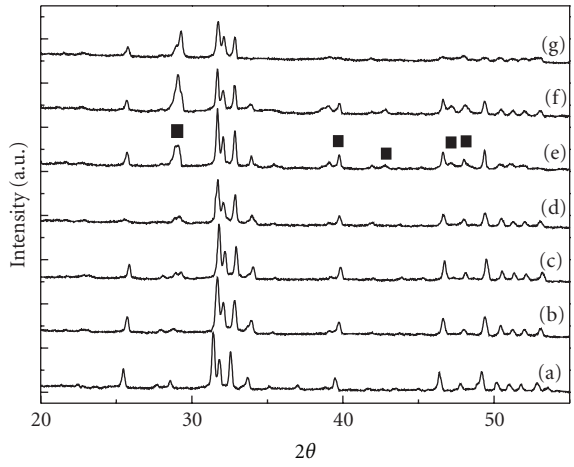

Figure 1: XRD patterns for sintered calcium phosphate pellets prepared in ratio of [Ca]/[P] = 1.50 and immersed in normal saline solution at 37°C for various lengths of time (■: $Ca_2P_2O_7$). (a) 0 d, (b) 2 d, (c) 4 d, (d) 7 d, (e) 14 d, (f) 28 d, and (g) 42 d.

the synthesized calcium phosphate powder pellets prepared in a ratio of [Ca]/[P] = 1.50 after the pellets had been sintered at 800°C for 4 h and immersed in a normal saline solution at 37°C for various lengths of time. Figure 1(a) shows the XRD pattern for the as-sintered sample. The pattern indicates that the pellet was composed of HA and rhenanite ($NaCaPO_4$) as the major and minor phases, respectively, and that no other phase(s) were detected. $NaCaPO_4$ had formed because of Na^+ ions interstitial to the apatite structure. The XRD pattern for the sample that had been immersed for 2 d is shown in Figure 1(b). Bragg's angle of all reflection peaks for HA had obviously shifted to high-angle sites. Although the degree of splitting of the (112) and (200) reflections of HA decreased, their intensity of the reflections did not change and no other phases had formed. Figure 1(c) shows the XRD pattern for the sintered calcium phosphate pellet prepared in a ratio of [Ca]/[P] = 1.50 and immersed for 4 d. The pattern reveals a new weaker reflection peak at $2\theta \approx 29.3°$. Nevertheless, all reflection peaks associated with HA have obviously shifted to higher angle sites, and the intensities of all the HA reflection peaks are slightly decreased. These phenomena occur because new substances form layers covering up previous ones on the surface of the pellet. The XRD pattern for the HA-sintered pellet immersed for 7 d is shown in Figure 1(d). Although the angles of the HA reflection peaks had returned to their original sites, the intensities of the HA reflection peaks were significantly decreased due to the intensity of the reflection peak associated with the new phase as well gradually obvious but the phase does not identify. Figure 1(e) shows the XRD pattern for the calcium phosphate pellet prepared in a ratio of [Ca]/[P] = 1.50 and immersed for 14 d. The pattern reveals that a new phase, calcium pyrophosphate ($Ca_2P_2O_7$; CPP, JCPDS card no. 73-0440), had formed on the surface of the pellet, and the intensities of the HA reflection peaks also returned to the same level as those of the as-sintered pellets because amorphous calcium phosphate (ACP) had been used as the precursor substance for CPP, resulting in the intensities of the HA reflection peaks decreasing and angle of peak-site shifting. However, no new reflection peaks appeared. The CPP crystals formed on the surface of the sintered calcium phosphate pellet immersed for 14 d then the sites of the HA reflection peaks returned to their original sites as in the pattern for the as-sintered pellet. Figure 1(f) shows the XRD pattern for the sintered calcium phosphate pellet prepared in a ratio of [Ca]/[P] = 1.50 and immersed in a normal saline solution at 37°C for 28 d. The intensities of CPP reflection peaks in this pattern were the highest because the increased thickness of the CPP crystallization layer led to further decrease in the intensity of the HA reflection peaks. The XRD patterns for the pellets immersed for 42 d are shown in Figure 1(g). Except for the successive decreases in the intensities of the HA reflection peaks, the intensities of CPP reflections also decrease.

3.2. Surface Morphologies of Immersed Sintered Calcium Phosphate Pellets Prepared in a Ratio of [Ca]/[P] = 1.50. The SEM images of the surface morphologies of the calcium phosphate powder synthesized in a ratio of [Ca]/[P] = 1.50, sintered at 800°C for 4 h , and immersed in a normal saline solution at 37°C for various lengths of time are shown in Figure 2. The surface morphology of the pellet immersed for 2 d is shown in Figure 2(a). A few of the HA grain boundaries appear blurred because the surface of the sintered sample is covered by an unknown substance. Figure 2(b) shows SEM image of the surface morphology of the sintered calcium phosphate sample immersed for 4 d. Amorphous substances were layered on the sample surface. The surface morphology of the sintered calcium phosphate sample immersed for 7 d is shown in Figure 2(c). A minute amount of irregular aggregated phase precipitate exists in addition to the amorphous substances on the surface. From the result shown in Figure 1(d), these amorphous substances and irregular aggregated phase precipitate correspond to the precursors of CPP and CPP crystallites, respectively. Figure 2(d) shows the SEM image of the surface morphology of the sintered calcium phosphate sample immersed in normal saline solution at 37°C for 14 d. The CPP crystallites were clearly observed and made the amorphous substance to discriminate against become to the area of slice join together. This phenomenon also caused the intensity of the HA reflection peaks to increases. The surface morphology of the sintered calcium phosphate pellet immersed for 28 d is shown in Figure 2(e). Although amorphous substances are not observed on the surface, the whole HA surface is covered by CPP, leading to a decrease in the intensities of HA the reflection peaks. Figure 2(f) shows the surface morphology of the sintered calcium phosphate sample immersed in a normal saline solution at 37°C for 42 d. The CPP has formed a linked flat-plane structure over the entire HA surface.

3.3. Variations in Postimmersion Concentration of Ca^{2+} Ions and Rate of Weight Loss of Sintered Calcium Phosphate Pellet Prepared in a Ratio of [Ca]/[P] = 1.50. In general, the Ca^{2+} ions in solution play the role of inducing phosphate

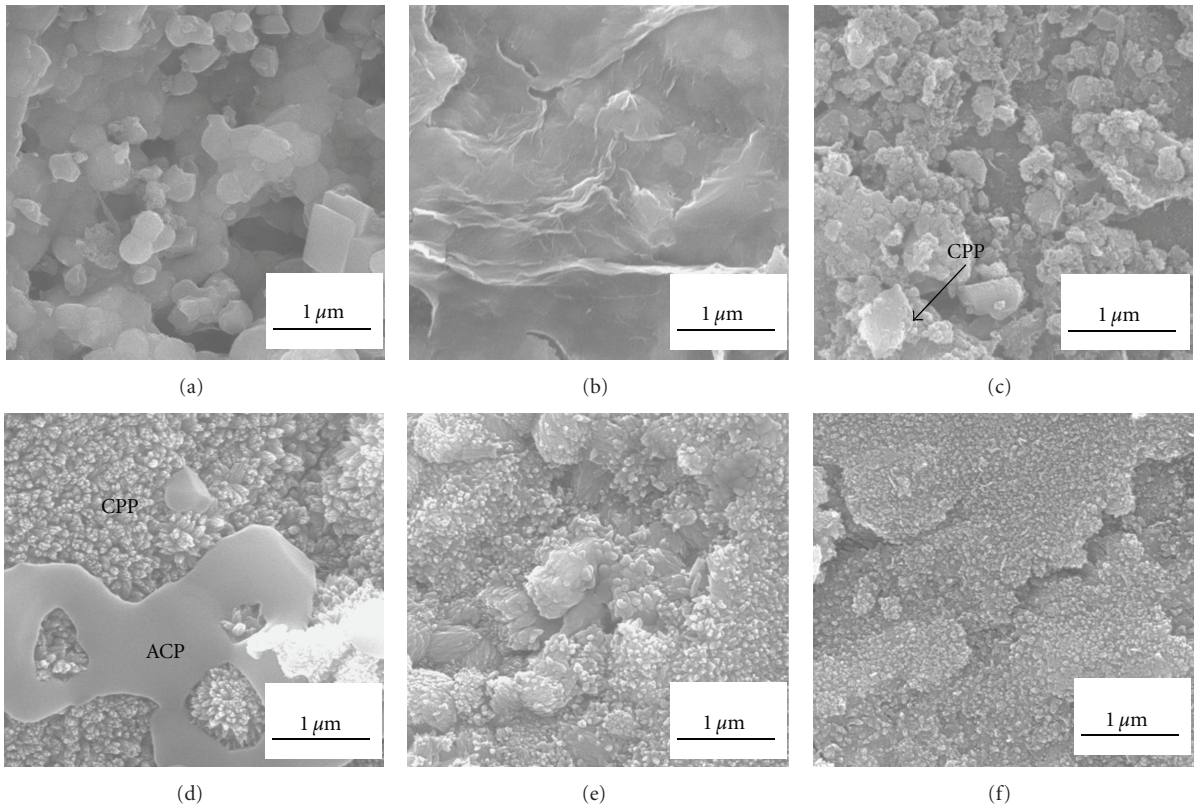

Figure 2: SEM images of microstructures on surface of sintered calcium phosphate pellets prepared in ratio of [Ca]/[P] = 1.50 and immersed in normal saline solution at 37°C for various lengths of time: (a) 2 d, (b) 4 d, (c) 7 d, (d) 14 d, (f) 28 d, and (f) 42 d.

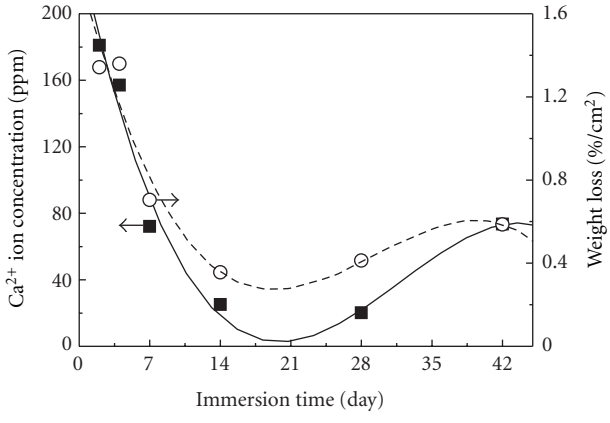

Figure 3: Concentration of Ca^{2+} ions and rate of weight loss of sintered calcium phosphate pellets immersed in normal saline solution at 37°C for various lengths of time.

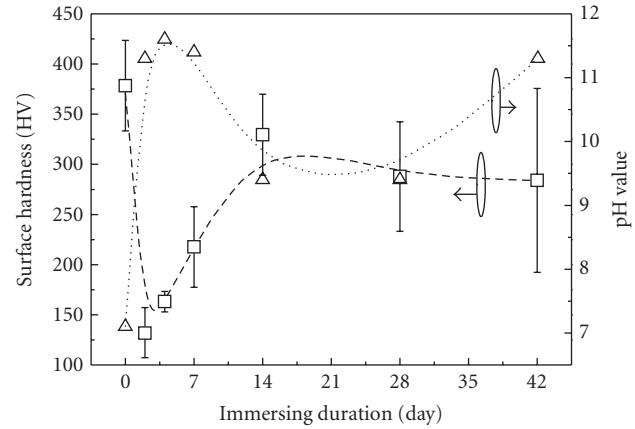

Figure 4: Surface hardness of sintered calcium phosphate pellets and pH of normal saline solutions in which pellets had been immersed at 37°C for various lengths of time.

precipitation. However, because of the presence of phosphorous (P) in the solution, the pH can change, possibly forming various ions such as $H_2PO_4^-$, HPO_4^{2-}, and PO_4^{3-}. Therefore, during immersion, except test the self change of HA sintered sample, variation in the solution composition is a significant contributor to the transformation of the sintered calcium phosphate samples. From the change in the Ca^{2+} concentration in the immersion solution measured using ICP-MS and the difference in the weight for sintered calcium phosphate sample measured before and after immersion, the variation in the sintered calcium phosphate samples during immersion can be investigated.

Figure 3 shows the variation in the concentration of Ca^{2+} ions and rate of weight loss per unit of surface area of sintered calcium phosphate samples prepared in the ratio of [Ca]/[P]

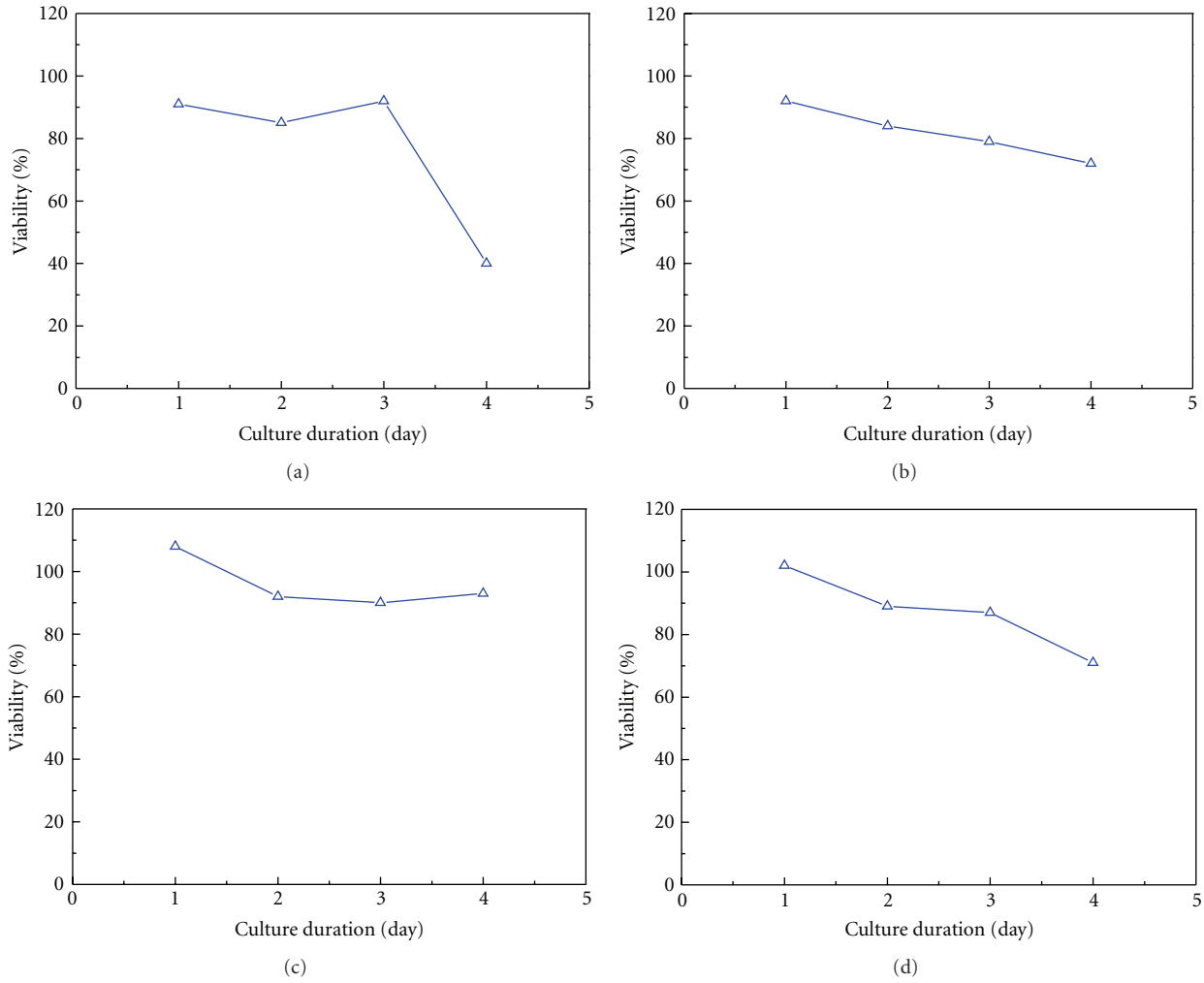

Figure 5: Viability of 3T3 cells cultured for various lengths of time in solutions of calcium phosphate powder extracted from pellets prepared in ratio of [Ca]/[P] = 1.50.

= 1.50 and immersed in a normal saline solution at 37°C for various lengths of time. The concentration of Ca^{2+} ions in the solution increased from 0 to 181 ppm, and the rate of weight loss per unit of surface area was 1.34%/cm^2 for the sample immersed for 2 d. This result indicates that the unstable calcium phosphate degraded and was released into the solution. When the immersion time increased to 14 d, the concentration of Ca^{2+} ions in the solution rapidly decreased and the rate of weight loss per unit of surface area decreased because the calcium phosphate product had reformed on the surface of the sintered calcium phosphate from the Ca^{2+} ions in the solution. This result is consistent with the XRD result and SEM observation for the amorphous substance precipitates. The concentration of Ca^{2+} ions in the solution gradually increased when the immersion time was longer than 14 d because the amorphous substance dissolved into the normal saline solution, and the CPP reformed. When the sintered calcium phosphate pellet was immersed for 42 d, the concentration of Ca^{2+} ions in the solution and the rate of weight loss of the sintered calcium phosphate pellet reached equilibrium. This result suggests that the equilibrium of the precipitation-dissolution reactions for ACP and CPP had approached completion.

3.4. The Variation in Pre- and Postimmersion Surface Hardness and pH of Immersion Solution after Sintered Calcium Phosphate Pellets Had Been Immersed for Various Lengths of Time. The variation in surface hardness and the pH of immersion solution for sintered calcium phosphate samples immersed for various amounts of time are shown in Figure 4. The minimum HV was 132.1 for the sample immersed for 2 d, suggesting that the ACP formed on the surface of the sintered calcium phosphate pellet prepared in a ratio of [Ca]/[P] = 1.50. The hardness values subsequently increased rapidly with increasing immersion time because of the CPP precipitate but could not reach the level of the pre-immersion sintered calcium phosphate sample. The surface hardness approached a stable value for the sample immersed for 14 d, and the sample surface exhibited a gradual tendency toward steady state.

Figure 4 also shows that the pH of the normal saline solution increases during the initial stage of immersion

because of the ACP precipitating and dissolving into the solution. The maximum pH of the normal saline solution reached 11.7 when the sintered calcium phosphate sample prepared in a ratio of [Ca]/[P] = 1.50 had been immersed for 4 d. Then the pH of the solution decreased for samples immersed longer than 4 days because CPP had formed, leading to a decrease in the concentrations of calcium and phosphor ions in the normal saline solution. For the sample immersed for 28 d, the pH of the solution increased, revealing that the calcium and phosphor ions were rereleased into the normal saline solution.

3.5. Biocompatibility of Calcium Phosphate Powder Pellets Prepared in the Ratio of [Ca]/[P] = 1.50 with regard to 3T3 Cells. The viability of 3T3 cells cultured for various lengths of time in solutions of calcium phosphate extracted from the pellets immersed for various lengths of time is shown in Figure 5. Figure 5(a) shows that the viability of the of 3T3 cells cultured in the solution of calcium phosphate extracted from the pellet immersed for 4 d is greater than 90% when the cells were cultured for 1 d. The high 3T3 cell viability is attributed to the addition of $CaCO_3$ to increase [Ca]/[P] ratio to one that was similar to that of stoichiometric HA [18]. This caused carbonate-substituted hydroxyapatite (CHA) to form, leading to increased biocompatibility. When the 3T3 cells were cultured for 4 d, their viability was still about 40%.

The viability of 3T3 cells cultured for various lengths of time in solutions of calcium phosphate extracted from the pellet immersed for 7 d are shown in Figure 5(b). It seems that the viability of 3T3 cells cultured in solutions prepared from calcium phosphate powders prepared in [Ca]/[P]=1.50 extracted from HA is greater than 70% for each culture time. Figure 5(c) shows the viability of 3T3 cells cultured in a solution prepared from HA powders prepared in [Ca]/[P]=1.50 extracted from the pellet immersed for 14 d. The viability remains above 90% for culture times from 1 to 4 d because the Ca^{2+} ions released from the test samples prevented the pH of the solution from decreasing, thereby increasing cell viability. When the HA powders prepared in [Ca]/[P]=1.50 after being immersed for 21 d, the cell viability of the extraction of HA powders for various culture times are shown in Figure 5(d). From Figure 5, the difference between the viability 3T3 cells cultured in solutions prepared from calcium phosphate extracted from HA powders with [Ca]/[P] = 1.5 and the viability of those cultured in solutions prepared from calcium phosphate extracted from HA powders with [Ca]/[P] = 1.0 decreases increasing immersion time of the pellets (data not shown). The results shown in Figure 5 also indicate that the HA powders with [Ca]/[P] = 1.5 exhibit higher biocompatibility because the [Ca]/[P] ratio approaches that of stoichiometric HA. Figure 6 shows the XRD pattern generated after cell culture for the precipitate from the HA-sintered pellet synthesized from DCPD and $CaCO_3$ prepared in a ratio of [Ca]/[P] = 1.50. The reflection peaks in the XRD pattern correspond to the CPP phase.

The morphologies of the 3T3 cells cultured on HA-sintered pellets prepared from DCPD and added $CaCO_3$ in the ratio of [Ca]/[P] = 1.50 are shown in Figure 7. Figure 7(a) shows optical microscopy (OM) image of the morphology of the cell adhesion on the bottom of the HA-sintered pellet after culturing for 4 d. Although the cells did not adhere to the bottom of the pellet, some precipitates had formed. The precipitates were identified as CPP, as shown in Figure 6. Figure 7(b) shows the enlarged view of Figure 7(a). The CPP precipitates consist of nonuniform polygons. The OM image of the morphology of the surrounding area on the sintered HA pellet is shown in Figure 7(c). The cell synapses were extended, and the cells exhibited interknit growth. This result may suggest that the release of ions during immersion of the sintered pellet had not affected the extended process of the normal mitosis of cells. Figure 7(d) shows the SEM image of the enlarged view of Figure 7(c). Some precipitates are surrounding the cells. From the preceding results and discussion, HA powders synthesized using DCPD and $CaCO_3$ as the starting materials in a ratio of [Ca]/[P] = 1.50 with hydrolysis can be good biomedical materials because they exhibit good biocompatibility.

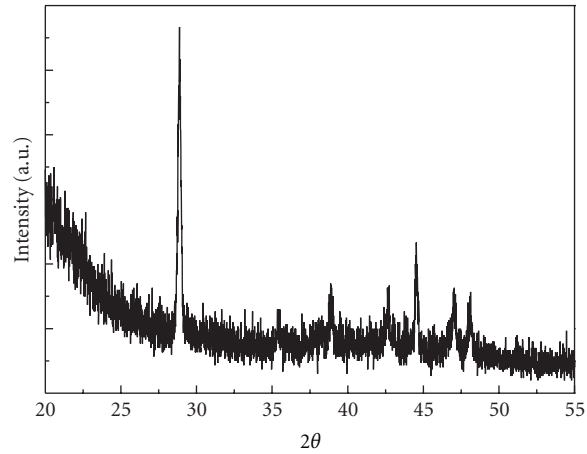

Figure 6: Post-cell-culture XRD pattern for precipitates of sintered calcium phosphate pellets prepared in ratio of [Ca]/[P] = 1.50.

4. Conclusions

The biocompatibility of HA-sintered pellets prepared in a ratio of [Ca]/[P] = 1.5 and powders prepared with various ratios of [Ca]/[P] were investigated using XRD, OM, SEM, ICP-MS, a pH meter, an immersion test, and a cell culture. When the HA-sintered pellet was immersed in a normal saline solution at 37°C for 4 d, XRD pattern exhibited a new weaker reflection peak at $2\theta \approx 29.3°$, and all the reflection peaks associated with HA shifted to higher-angle sites; however, the intensities of all the HA reflection peaks slightly decreased. The CPP phase was formed on the surface of the pellets after the pellets had been immersed in the normal saline solution for 42 d. The SEM image of the surface morphology showed that amorphous precursors of CPP and irregular aggregated CPP crystallites had formed after the pellets had been immersed in the normal saline solution for 14 d. The CPP formed a linked flat-plane

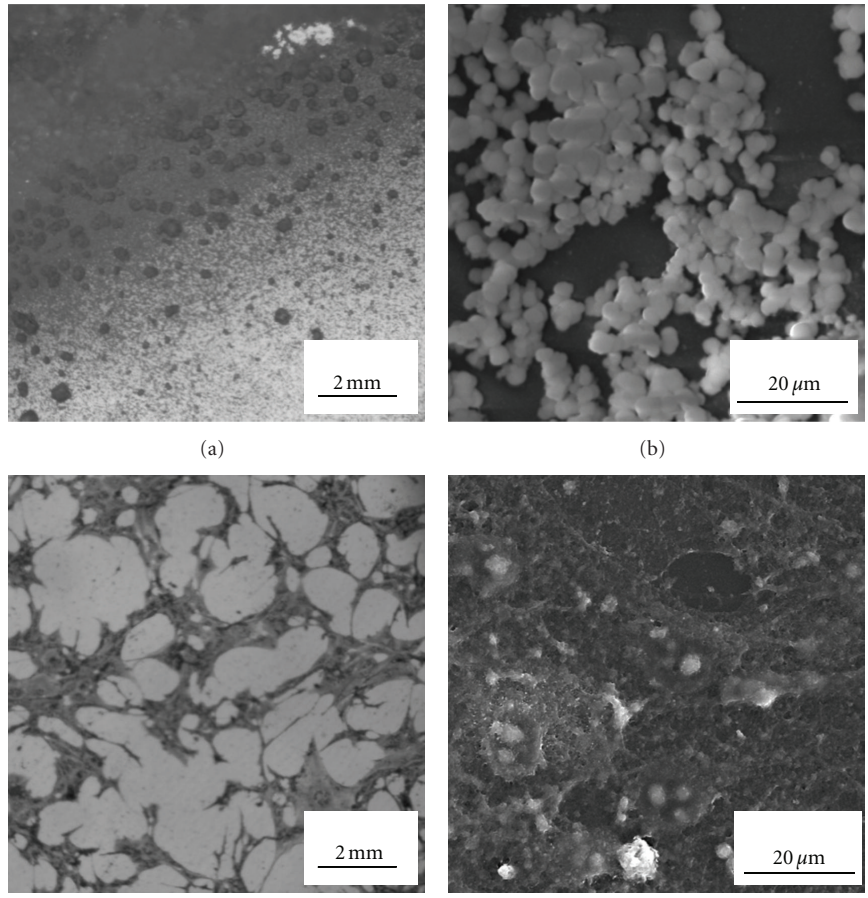

Figure 7: Morphologies of cells cultured on sintered calcium phosphate pellets prepared in ratio of [Ca]/[P] = 1.50: (a) OM image of precipitates, (b) SEM image of precipitates, (c) OM image of cell growth, and (d) SEM image of cell growth.

structure over the entire HA surface after the pellet had been immersed in a normal saline solution at 37°C for 42 d. In addition, when the pellet had been immersed in the normal saline solution for 42 d, the concentration of Ca^{2+} ions in the solution, and the rate of weight loss of the HA-sintered pellet reached an equilibrium because the precipitation-dissolution reactions for ACP and CPP had approached completion. The minimum surface hardness of HA was 132.1 because the ACP had formed on the HA-sintered sample immersed for only 2 d. The surface hardness then rapidly increased because of the CPP precipitate but could not reach to the level of hardness of sintered HA pellet before immersion. The maximum pH of the normal saline solution was 11.7 when the HA-sintered pellet had been immersed for 4 d. The viability of 3T3 cells remained above 90% for culture duration from 1 to 4 d with extracts of HA powders having [Ca]/[P] = 1.50 after the pellets had been immersed in a normal saline solution for 14 d. The HA-sintered pellet was prepared in a ratio of [Ca]/[P] = 1.50 after the cells had cultured for 4 d. Although the cells did not adhere on the bottom of the pellet, some CPP precipitate had formed. The morphology of the surrounding area on the HA-sintered pellet after the cells had cultured for 4 d shows that the cell synapses were extended and that the cells exhibited interknit growth. Therefore, we suggest that HA powders synthesized using CPP and $CaCO_3$ in the ratio [Ca]/[P] = 1.50 with hydrolysis can be good biomedical materials because they exhibit good biocompatibility.

Acknowledgments

The authors gratefully acknowledge the financial support provided by the National Science Council of the Republic of China (Taiwan) under contract no. NSC 97-2221-E-037-001-MY3. The authors also gratefully acknowledge Mr. F. C. Wu and Mr. H. Y. Yao for their help with SEM and TEM imaging, respectively, when preparing the manuscript.

References

[1] S. Kannan, A. F. Lemos, J. H. G. Rocha, and J. M. F. Ferreira, "Characterization and mechanical performance of the Mg-stabilized β-$Ca_3(PO_4)_2$ prepared from Mg-substituted Ca-deficient apatite," *Journal of the American Ceramic Society*, vol. 89, no. 9, pp. 2757–2761, 2006.

[2] A. Bandyopadhyay, S. Bernard, W. Xue, and S. Böse, "Calcium phosphate-based resorbable ceramics: influence of MgO, ZnO, and SiO_2 dopants," *Journal of the American Ceramic Society*, vol. 89, no. 9, pp. 2675–2688, 2006.

[3] S. S. Banerjee, S. Tarafder, N. M. Davies, A. Bandyopadhyay, and S. Bose, "Understanding the influence of MgO and SrO binary doping on the mechanical and biological properties of β-TCP ceramics," *Acta Biomaterialia*, vol. 6, no. 10, pp. 4167–4174, 2010.

[4] L. L. Hench, "Bioceramics," *Journal of the American Ceramic Society*, vol. 81, no. 7, pp. 1705–1728, 1998.

[5] J. M. Gomez-Vega, E. Saiz, A. P. Tomsia, G. W. Marshall, and S. J. Marshall, "Bioactive glass coatings with hydroxyapatite and Bioglass® particles on Ti-based implants. 1. Processing," *Biomaterials*, vol. 21, no. 2, pp. 105–111, 2000.

[6] M. Swetha, K. Sahithi, A. Moorthi, N. Srinivasan, K. Ramasamy, and N. Selvamurugan, "Biocomposites containing natural polymers and hydroxyapatite for bone tissue engineering," *International Journal of Biological Macromolecules*, vol. 47, no. 1, pp. 1–4, 2010.

[7] G. K. Lim, J. Wang, S. C. Ng, and L. M. Gan, "Processing of fine hydroxyapatite powders via an inverse microemulsion route," *Materials Letters*, vol. 28, no. 4–6, pp. 431–436, 1996.

[8] W. Suchanek and M. Yoshimura, "Processing and properties of hydroxyapatite-based biomaterials for use as hard tissue replacement implants," *Journal of Materials Research*, vol. 13, no. 1, pp. 94–117, 1998.

[9] M. Swetha, K. Sahithi, A. Moorthi et al., "Synthesis, characterization, and antimicrobial activity of nano-hydroxyapatite-zinc for bone tissue engineering applications," *Journal of Nanoscience and Nanotechnology*, vol. 12, pp. 167–172.

[10] J. Chen, Q. Yu, G. Zhang, S. Yang, J. Wu, and Q. Zhang, "Preparation and biocompatibility of nanohybrid scaffolds by in situ homogeneous formation of nano hydroxyapatite from biopolymer polyelectrolyte complex for bone repair applications," *Colloids and Surfaces B*, vol. 93, pp. 100–107, 2012.

[11] I. Brook, C. Freeman, S. Grubb et al., "Biological evaluation of nano-hydroxyapatite-zirconia (HA-ZrO_2) composites and strontium-hydroxyapatite (Sr-HA) for load-bearing applications," *Journal of Biomaterials Applications*, vol. 27, no. 3, pp. 291–298, 2012.

[12] Y. Li, J. De Wijn, C. P. A. T. Klein, S. Van de Meer, and K. De Groot, "Preparation and characterization of nanograde osteoapatite-like rod crystals," *Journal of Materials Science*, vol. 5, no. 5, pp. 252–255, 1994.

[13] G. Munir, G. Koller, L. Di Silvio, M. J. Edirisinghe, W. Bonfield, and J. Huang, "The pathway to intelligent implants: osteoblast response to nano silicon-doped hydroxyapatite patterning," *Journal of the Royal Society Interface*, vol. 8, no. 58, pp. 678–688, 2011.

[14] D. B. Haddow, P. F. James, and R. Van Noort, "Characterization of sol-gel surfaces for biomedical applications," *Journal of Materials Science*, vol. 7, no. 5, pp. 255–260, 1996.

[15] K. Hwang and Y. Lim, "Chemical and structural changes of hydroxyapatite films by using a sol-gel method," *Surface and Coatings Technology*, vol. 115, no. 2-3, pp. 172–175, 1999.

[16] K. Ohta, M. Kikuchi, J. Tanaka, and H. Eda, "Synthesis of c axes oriented hydroxyapatite aggregate," *Chemistry Letters*, vol. 9, pp. 894–895, 2002.

[17] W. J. Shih, Y. F. Chen, M. C. Wang, and M. H. Hon, "Crystal growth and morphology of the nano-sized hydroxyapatite powders synthesized from $CaHPO_4 \cdot 2H_2O$ and $CaCO_3$ by hydrolysis method," *Journal of Crystal Growth*, vol. 270, no. 1-2, pp. 211–218, 2004.

[18] W. J. Shih, M. C. Wang, and M. H. Hon, "Morphology and crystallinity of the nanosized hydroxyapatite synthesized by hydrolysis using cetyltrimethylammonium bromide (CTAB) as a surfactant," *Journal of Crystal Growth*, vol. 275, no. 1-2, pp. e2339–e2344, 2005.

[19] S. Ban and J. Hasegawa, "Morphological regulation and crystal growth of hydrothermal-electrochemically deposited apatite," *Biomaterials*, vol. 23, no. 14, pp. 2965–2972, 2002.

[20] S. K. Yen and C. M. Lin, "Cathodic reactions of electrolytic hydroxyapatite coating on pure titanium," *Materials Chemistry and Physics*, vol. 77, no. 1, pp. 70–76, 2003.

[21] W. J. Shih, Y. H. Chen, S. H. Wang, W. L. Li, M. H. Hon, and M. C. Wang, "Effect of $NaOH_{(aq)}$ treatment on the phase transformation and morphology of calcium phosphate deposited by an electrolytic method," *Journal of Crystal Growth*, vol. 285, no. 4, pp. 633–641, 2005.

[22] M. C. Wang, W. J. Shih, K. M. Chang, S. H. Wang, W. L. Li, and H. H. Huang, "Effect of process parameters on the crystallization and morphology of calcium phosphate at a constant pressure of 80 Torr," *Journal of Non-Crystalline Solids*, vol. 356, no. 31-32, pp. 1546–1553, 2010.

[23] W. J. Shih, M. C. Wang, K. M. Chang et al., "Phase transformation of calcium phosphates by electrodeposition and heat treatment," *Metallurgical and Materials Transactions A*, vol. 41, pp. 3509–3516, 2010.

[24] W. Pon-On, S. Meejoo, and I. M. Tang, "Formation of hydroxyapatite crystallites using organic template of polyvinyl alcohol (PVA) and sodium dodecyl sulfate (SDS)," *Materials Chemistry and Physics*, vol. 112, no. 2, pp. 453–460, 2008.

[25] T. Ma, Z. Xia, and L. Liao, "Effect of reaction systems and surfactant additives on the morphology evolution of hydroxyapatite nanorods obtained via a hydrothermal route," *Applied Surface Science*, vol. 257, no. 9, pp. 4384–4388, 2011.

[26] H. El Feki, J. M. Savariault, and A. B. Salah, "Structure refinements by the Rietveld method of partially substituted hydroxyapatite: $Ca_9Na_{0.5}(PO_4)_{4.5}(CO_3)_{1.5}(OH)_2$," *Journal of Alloys and Compounds*, vol. 287, no. 1-2, pp. 114–120, 1999.

[27] E. A. P. De Maeyer, R. M. H. Verbeeck, and D. E. Naessens, "Stoichiometry of Na^+- and CO_3I^--containing apatites obtained by hydrolysis of monetite," *Inorganic Chemistry*, vol. 32, no. 25, pp. 5709–5714, 1993.